Figure legends supplemental figures

Supplemental figure 1.

(**a**) Staining pattern of cre-protein is similar to GFAP-staining of astrocytes but does not resemble NeuN-staining of neurons in mouse hippocampus. (**b**) Cre protein does not colocalize with NeuN-positve neurons (scalebar 100μm) (**c**) Upper: GFAPcre+/VHL$^{+f/+f}$ are smaller than widtype littermates. Lower: A dome-shaped head in GFAPcre+/VHL$^{+f/+f}$ mice (arrowhead) indicates the presence of hydrocephalus in those animals. (**d**) Analysis of Evans blue (EB) leakage into the CNS indicates a significantly impaired blood-brain barrier function in GFAPcre+/VHL$^{+f/+f}$ (1.73 ± 0.2-fold increase (n=7) of OD_{620}/g brain) and GFAPcre+/VHL$^{+f/+f}$/HIF-1α$^{+f/+f}$ (1.46 ± 0.2-fold increase (n=4)) compared to GFAPcre-negative mice. GFAPcre+/VHL$^{+f/+f}$/HIF-2α$^{+f/+f}$ mice have no significantly altered blood-brain barrier permeability (1.22 ± 0.1-fold change (n=5; Mann-Whitney-test)) (**e**) Upper graph: hearts of GFAPcre+/VHL$^{+f/+f}$ (167.1 ± 10.8 mg (n=7)) and of GFAPcre+/VHL$^{+f/+f}$/HIF-1α$^{+f/+f}$ (158.0 ± 7.9 (n=5)) are significantly larger than hearts of control (GFAPcre-; 130.0 ± 2.5 mg (n=9)) and of GFAPcre+/VHL$^{+f/+f}$/HIF-2α$^{+f/+f}$ mice (135.0 ± 8.9 mg (n=4; Mann-Whitney-test)). Lower graph: spleens are significantly enlarged in GFAPcre+/VHL$^{+f/+f}$ (244.2 ± 31.9 mg (n=6)) and in GFAPcre+/VHL$^{+f/+f}$/HIF-1α$^{+f/+f}$ animals (173.0 ± 14.5 mg (n=5)) compared to control mice (GFAPcre-: 77.7 ± 8.4 mg (n=9)). Spleens are not significantly different in GFAPcre+/VHL$^{+f/+f}$/HIF-2α$^{+f/+f}$ animals (88 ± 0.01 mg (n=4); data represents means ± S.E.M.). (**f**) Hydrocephaly is detectable in three week old GFAPcre+/VHL$^{+f/+f}$ and GFAPcre+/VHL$^{+f/+f}$/HIF-1α$^{+f/+f}$ animals. In GFAPcre+/VHL$^{+f/+f}$/HIF-2α$^{+f/+f}$ mice ventricles are not enlarged (representative Nissl staining, 50x magnification).

Supplemental figure 2.

Expression of VEGF mRNA (**a**) and GLUT-1 mRNA (**b**) in livers is not significantly different between control (GFAPcre-; n=11), GFAPcre+/VHL$^{+f/+f}$ (n=6), GFAPcre+/VHL$^{+f/+f}$/HIF-1$\alpha^{+f/+f}$ (n=6) and GFAPcre+/VHL$^{+f/+f}$/HIF-2$\alpha^{+f/+f}$ (n=5) animals (data represents means ± S.E.M.). (**c**) VEGF mRNA is significantly upregulated in brains of GFAPcre+/VHL$^{+f/+f}$ (n=10) and GFAPcre+/VHL$^{+f/+f}$/HIF-1$\alpha^{+f/+f}$ mice (n=6) compared to control animals (GFAPcre-; n=8). Double knockout of VHL and HIF-1α does not change VEGF expression significantly. In contrast, double knockout of VHL and HIF-2α (n=10) significantly reduces VEGF upregulation, and double knockout of VHL and VEGF (n=5) reduces it further to wildtype levels (data represent means ± S.E.M.). (**d**) Immunofluorescence staining in the hippocampus shows that VEGF upregulation in GFAPcre+/ GFAPcre+/VHL$^{+f/+f}$ mice increases vessel numbers as visualized by the endothelial marker CD34 (red). Double knockout of VHL and HIF-2α reduces vessel numbers whereas double knockout of VHL and HIF-1α has essentially no effect. In GFAPcre+/VHL$^{+f/+f}$/VEGF$^{+f/+f}$ mice vessel number is further reduced (representative picture of 3 animals each genotype; astrocytes are stained with anti-GFAP (green); nuclei are stained with DAPI; scalebars 100μm). (**e**) 2-Photon microscopy shows the increased cerebral vessel number in GFAPcre+/VHL$^{+f/+f}$ and GFAPcre+/VHL$^{+f/+f}$/HIF-1$\alpha^{+f/+f}$ mutant animals. No difference is observed between wildtype and GFAPcre+/VHL$^{+f/+f}$/HIF-2$\alpha^{+f/+f}$ animals (representative images of cranial windows; larger image 400x, scalebar 50μm; inset 200x, scalebar 200μm). (**f**) In vivo measurements of brain capillary diameter (right) and the blood velocity in the brain capillaries (left) by 2-photon microscopy

demonstrate that both GFAPcre+/VHL$^{+f/+f}$ and GFAPcre+/VHL$^{+f/+f}$/HIF-1$\alpha^{+f/+f}$ animals have significantly thicker capillaries and that bloodflow is significantly slower compared to wildtype (GFAPcre-) and GFAPcre+/VHL$^{+f/+f}$/HIF-2$\alpha^{+f/+f}$ mice (n=4 each genotype; Kruskal-Wallis-test).

Supplemental figure 3.

(**a**) Survival of GFAPcre+/VHL$^{+f/+f}$/VEGF$^{+f/+f}$ mice (n=19) is significantly reduced compared to wildtype mice (GFAPcre-; n=62), but extended compared to GFAPcre+/VHL$^{+f/+f}$ animals (data represents median survival (weeks)). (**b**) The hydrocephaly of the GFAPcre+/VHL$^{+f/+f}$ mice is completely rescued in GFAPcre+/VHL$^{+f/+f}$/VEGF$^{+f/+f}$ double knockout animals (representative T1 weighed fMRI picture).

Supplementary Methods:

Primer Sequences for RNA analyses:
EPO: (F): 5′-TGCGACAGTCGAGTTCTGGA-3′
(R): 5′-TCTGCACAACCCATCGTGAC-3′
Probe: 5′- (6~FAM)AGGTACATCTTAGAGGCCAAGGAGGCAGAAA-(BHQ)-3′

VEGF (F): 5′-ATCCGCATGATCTGCATGG-3′
(R): 5′-AGTCCCATGAAGTGATCAAGTTCA-3′
Probe: 5′-(6~FAM)TGCCCACGTCAGAGAGCAACATCAC-(BHQ)-3′

Primer Sequences for DNA recombination analyses:
Location of the primers see (42)
VHL:
VHL F1: 5′-CTGGTACCCACGAAACTGTC-3′
VHL F2: 5′-CTAGGCACCGAGCTTAGAGGTTTGCG-3′
VHL R: 5′-CTGACTTCCACTGATGCTTGTCACAG-3′
Product size: VHL 2-lox allele: 460bp, 1-lox allele: 260bp; wt allele 290bp

HIF-1α:
HIF-1α F1: 5′-TTGGGGATGAAAACATCTGC-3′
HIF-1α F2: 5′-GCAGTTAAGAGCACTAGTTG-3′
HIF-1α R: 5′-GGAGCTATCTCTCTAGACC-3′
Product size: HIF-1α 1-lox allele: 270bp; 2-lox allele 260bp; wt allele 240bp

HIF-2α:
HIF-2α F1: 5′-CAGGCAGTATGCCTGGCTAAT TCCAGTT-3′
HIF-2α F2: 5′-CTTCTTCCATCATCTGGGATCTGGGACT-3′
HIF-2α R: 5′-GCTAACACTGTACTGTCTGAAAGAGTAGC-3′
Product size: HIF-2α 1-lox allele: 360bp; 2-lox allele 460bp; wt allele 430bp

Supplemental Figure 1

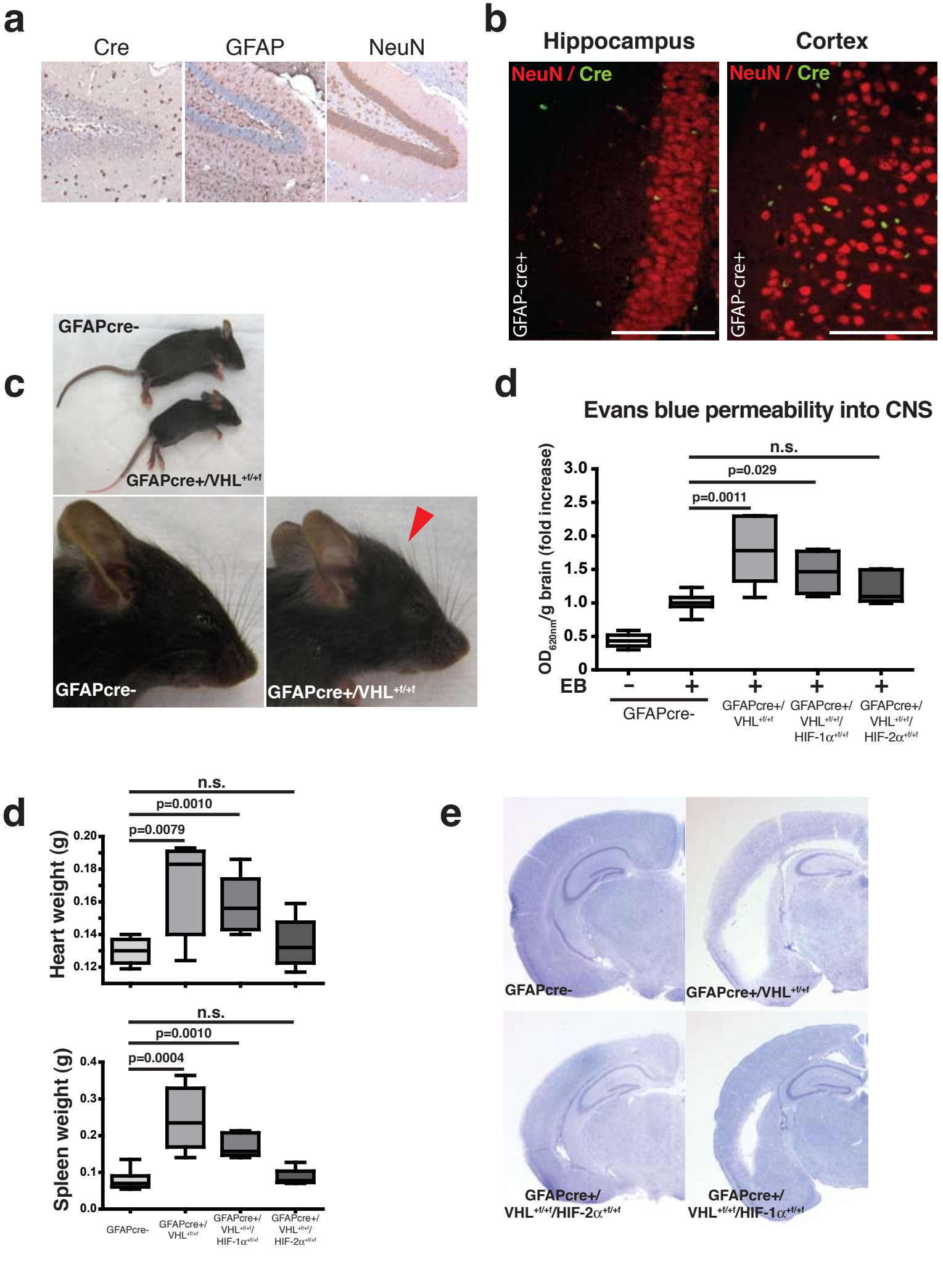

Supplemental Figure 2

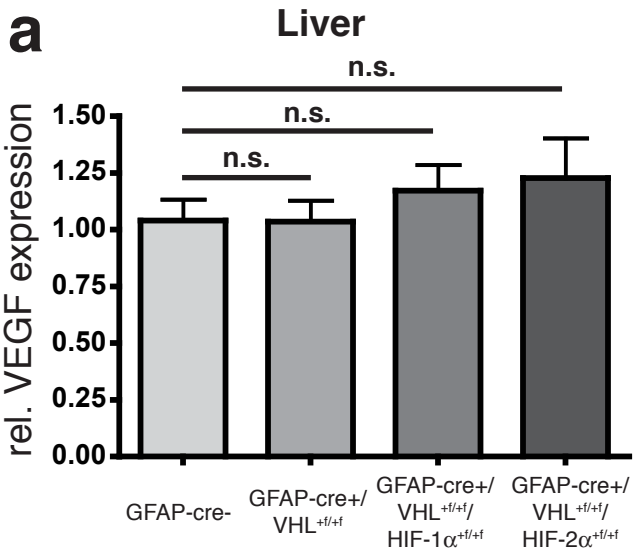

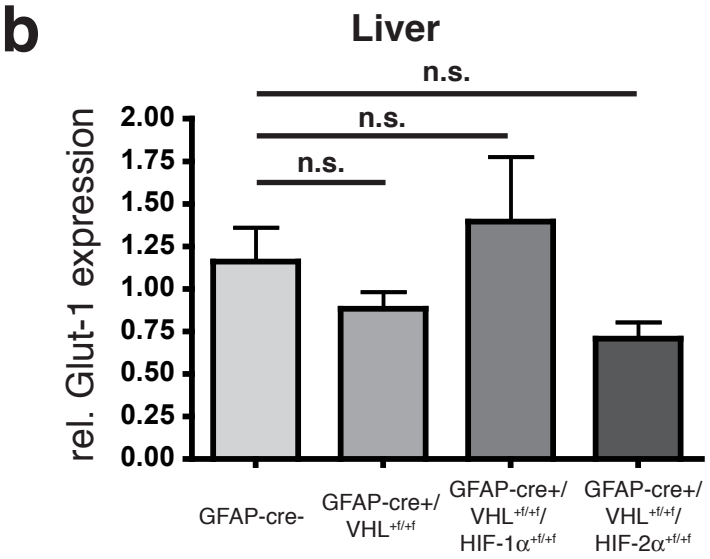

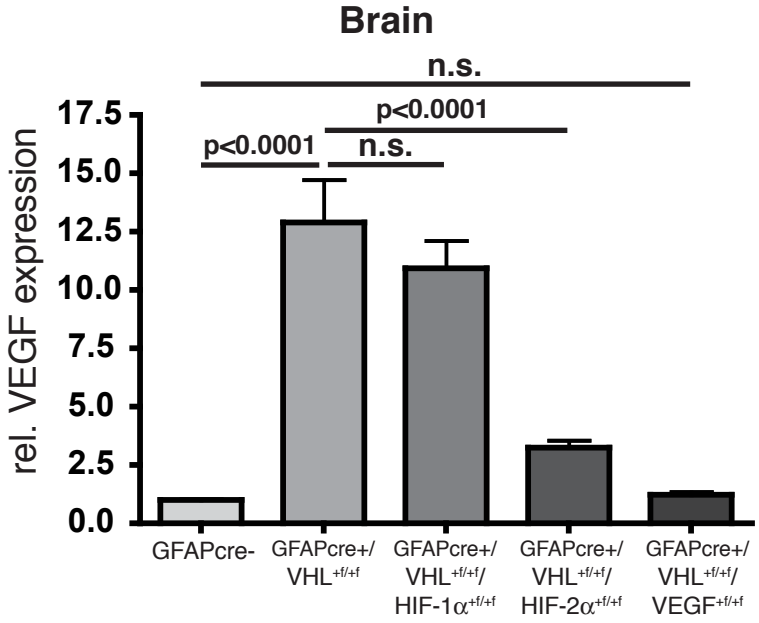

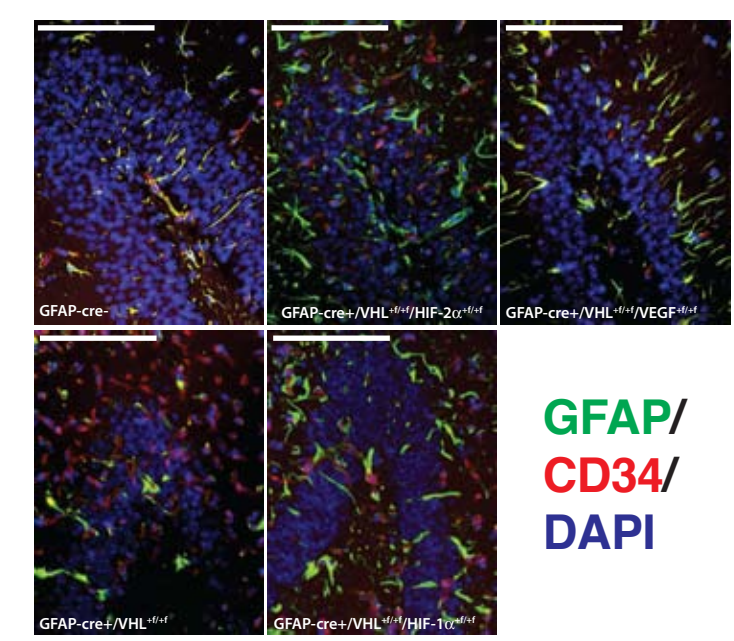

Supplemental Figure 2

e

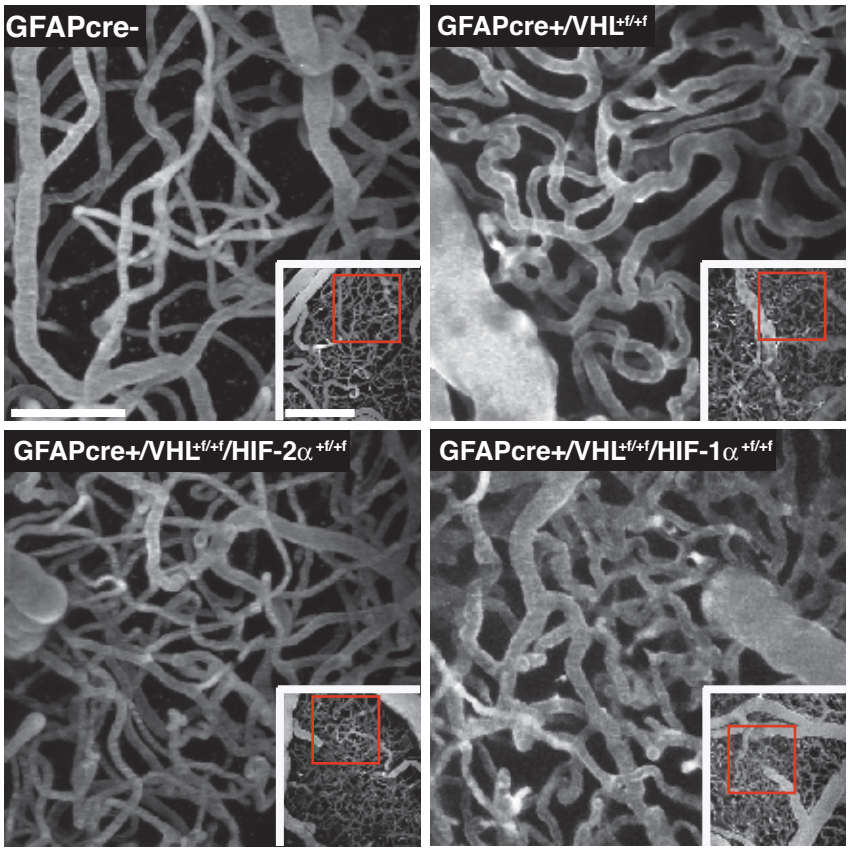

f

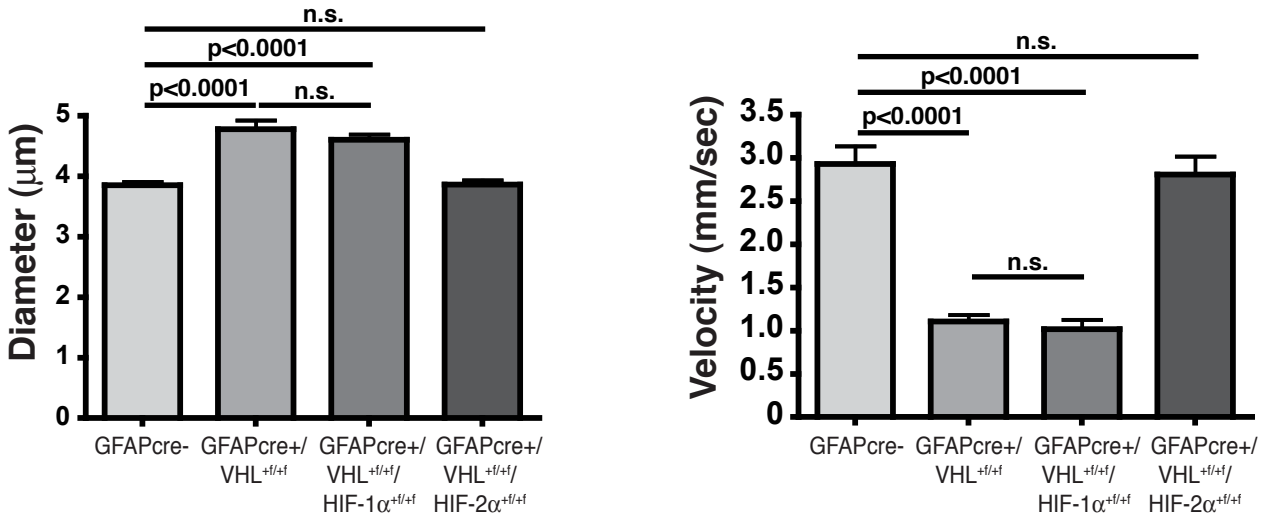

Supplemental figure 3